GEOPHYSICAL RESEARCH LETTERS, VOL. 25, NO. 22, PAGES 4109-4112, NOVEMBER 15, 1998

First detection of a terrestrial MeV X-ray burst

J.E. Foat[1,2,3], R.P. Lin[1,3], D.M. Smith[1], F. Fenrich[1], R. Millan[1,3], I. Roth[1], K.R. Lorentzen[4], M.P. McCarthy[4], G.K. Parks[4], J.P. Treilhou[5]

Abstract. We report the first detection of a terrestrial X-ray burst extending up to MeV energies, made by a liquid-nitrogen-cooled germanium detector (~ 2 keV FWHM resolution) on a high-altitude balloon at 65.5° magnetic latitude (L=5.7) in the late afternoon (1815 MLT) during low geomagnetic activity. The burst occurred at 1532-1554 UT on August 20, 1996, and consisted of seven peaks of ~60-90 s duration, spaced by ~100-200 s, with quasi-periodic (~10-20 s) modulation of the peak count rates. The very hard X-ray spectrum extends to the instrumental limit of 1.4 MeV, and is consistent with bremsstrahlung emission from monoenergetic, ~1.7 MeV, precipitating electrons. Since the trapped relativistic electrons showed a steeply falling energy spectrum from 0.6 to 4 MeV (at L=6.6), the precipitation mechanism appears to be highly energy selective. The modulation frequencies suggest scattering of the MeV electrons due to gyro-resonance with Doppler-shifted electromagnetic ion cyclotron waves, but either equatorial proton densities a factor of ~10^2 higher than typical for the plasmasphere or significant O^+ densities would be required.

Introduction

Hard > ~ 20 keV X-rays from the bremsstrahlung emission of energetic electrons precipitating into the atmosphere were first detected from a balloon by *Winckler et al. [1958]*. Subsequent balloon measurements have established that even in the absence of geomagnetic activity (*Anderson and Enemark, 1960*), an average X-ray flux of ~15 $cm^{-2}s^{-1}$ is present in the auroral zone > 50% of the time (*Anderson, 1965*). Periods of intense X-ray emission (up to several hundred $cm^{-2}s^{-1}$) lasting from several minutes to several hours, often accompany geomagnetic disturbances (for a review see *Parks et al., 1993*). These events show rich temporal structure on time scales from ~5 ms (*Parks et al., 1967*) to several minutes (*Evans, 1965*).

The energy spectrum of the X-rays typically drops off rapidly between 20-200 keV with e-folding energies of ~20-30 keV (see, for example, *Smith et al., 1995*), but on rare occasions significant fluxes are detected above 120 keV with e-folding energies of ~200 keV (*Parks et al., 1979*). To our knowledge, the highest energy previously detected in terrestrial X-rays is ~500 keV, by a spacecraft-borne detector (*Imhof et al., 1978*).

Precipitating MeV energy electrons, however, are often detected near the trapping boundary in narrow latitude bands up to 2-3 degrees wide, which are detected by low-Earth-orbiting (LEO) spacecraft as a few s to ~30 s spikes (*Blake et al., 1996*). Intense MeV electron precipitation can deposit energy at rates up to 3-4 orders of magnitude larger than that due to cosmic rays and solar EUV radiation at altitudes of 40-70 km; this can provide coupling from the magnetosphere into the middle atmosphere, and possibly even affect atmospheric ozone chemistry (*Baker et al., 1987*).

Here we present high spectral resolution balloon observations of the most energetic terrestrial hard X-ray burst ever detected. The nearly stationary balloon platform allows the temporal evolution of the entire precipitation event to be observed.

Observations

The observations were made with a liquid nitrogen cooled, 5.5 cm diam x 5.5 cm coaxial germanium detector (GeD), which had flown previously on an Antarctic long duration (~9 day) balloon flight [*Smith et al., 1995*]. The GeD inner bore is electrically segmented to form two detectors: D0, which occupies a few cm^3 at the center of the top surface, and D1 with the rest of the ~130 cm^3 volume. D1 covers from ~20 keV to 1.365 MeV with ~2 keV FWHM resolution. Its effective photopeak area (at vertical incidence) is 6 cm^2 at 26 keV, 11 cm^2 at 81 keV, 7 cm^2 at 356 keV, and 2.5 cm^2 at 1.115 MeV. A 0.54 cm thick lead collimator limits the field of view to a 45° half-angle vertical cone.

At count rates below 500 c/s, every energy deposition in D0 and D1 was measured with 12 bit precision (4096 channels with 0.337 keV per channel) and telemetered to the ground. Above 500 c/s, the energy depositions in D1 were binned into 96 channel spectra every 1/8 s, with channel widths increasing quasi-logarithmically from 2.7 keV at 20 keV to 42.9 keV at 1.365 MeV; only these spectra, together with >40 keV and <40 keV D1 counts every 10 ms, were telemetered.

The GeD was flown together with an X-ray imager (XRI), broad band X-ray detectors, VLF sensors, and tri-axial electric and magnetic field sensors, on the first flight of INTERBOA (INTERball and Balloon Observations of Aurora), an international campaign to study particle acceleration processes and the coupling of solar, magnetospheric, and ionospheric activity. The balloon was launched at ~1000 UT on August 19, 1996 from the ESRANGE facility in Kiruna, Sweden, and stayed aloft for nearly 40 hours at float altitudes between 32.5 km and 35 km. Magnetic activity was low (Kp~2, D_{st}~ -10 nT), and during the first 30 hours the D1 count rate stayed close to background.

[1] Space Sciences Laboratory, University of California, Berkeley CA 94720-7450

[2] Presently, at the Green Institute of Geophysics and Planetary Physics, University of California, San Diego, CA 92093

[3] Also Physics Department, University of California, Berkeley, CA 94720

[4] Geophysics Program, AK 50, University of Washington, Seattle, WA 98195

[5] Center d'Etude Spatiale des Rayonnements, B.P. 4346, 31209 Toulouse Cedex, France

Paper number 1998GL900134.
0094-8276/98/1998GL900134$05.00

An intense hard X-ray burst was detected at 1532 UT (1815 MLT) when the balloon was at 117.6 E, 65.5 N magnetic (L=5.7) with ~6 g/cm^2 of overlying atmosphere. The >20 keV D1 count rate (Figure 1a, upper) exhibited a series of seven smooth peaks, reaching a maximum of ~ 2400 c/s at 1547 UT. The peak durations (FWHM) ranged from ~60 to ~90 s and the time between peaks varied from 105 s (peaks 2 and 3) to 225 s (peaks 3 and 4). The count rate then returned smoothly to background by 1555 UT.

The tops of the peaks show fast, quasi-periodic (~10-20 s) modulations of up to ~10% of the total count rate (e.g. at ~1546 UT). These are more evident in the residual (1 s) count rate (Figure 1a, bottom) obtained by subtracting a 20 s running average. Power spectra of the residual count rate were obtained every 5 s, using a Fast Fourier Transform (FFT) routine supplied with the IDL software package. To match the approximate duration of the modulation, the FFT window was chosen to be 35 s long, resulting in 17 frequency bands centered on 28.6 mHz, 57.1 mHz, ..., 486 mHz.

To identify significant contributions in a particular FFT, a statistically equivalent data set without significant periodicities was constructed by summing the count rate during pre-event background over a fixed interval chosen to provide the same average number of counts per bin as seen in that FFT window. A 20 bin running average was then subtracted from this data set, and the same FFT analysis performed on the residual rate. The resulting distribution of spectral power was used to define the 1σ standard deviation power level.

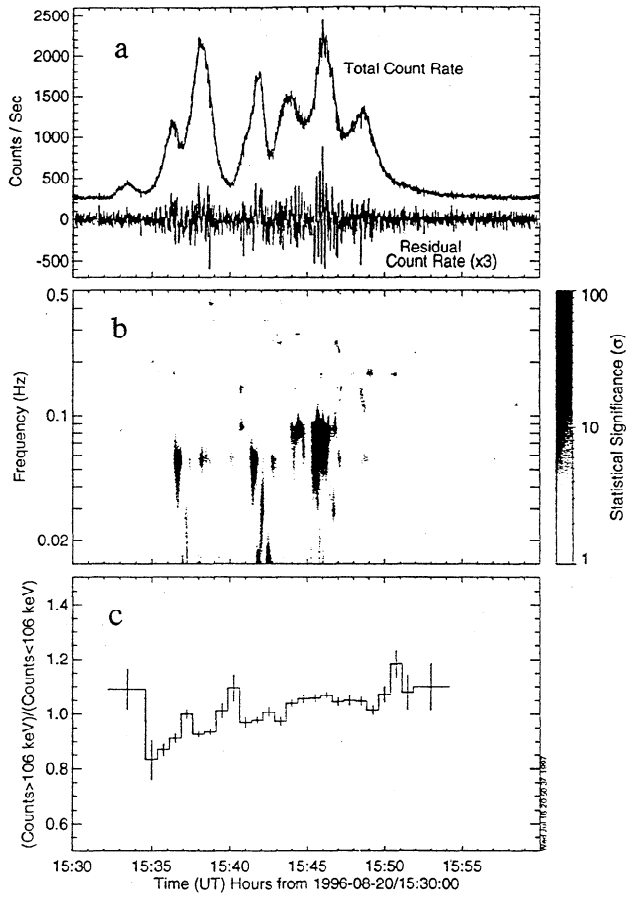

Figure 1. Relativistic electron precipitation event of August 20, 1996. (a) The upper trace is the 1 s average of the > 20 keV count rate. The lower trace is the residual count rate after a 20 s running average has been removed. (b) Dynamic spectral analysis of the residual count rate. A Fast Fourier Transform (FFT) with a 35 s window is plotted every 5 s in units of the standard deviation σ for that FFT window. (c) The (background subtracted) ratio of counts between 20 keV to 106 keV to those between 106 keV and 1.365 MeV.

Figure 1b plots the spectral power in terms of the σ for each FFT window. Significant (>3σ) modulation is observed around 57.1 mHz before ~1544 UT (10 σ, 7 σ, 20 σ, respectively for peaks 2, 3, 4), shifting to around 85.7 mHz after (20 and ~100 σ for peaks 5 and 6), but peaks 1 and 7 show no significant modulation. Significant power at frequencies lower than 57.1 mHz appears only at ~1542 UT, when the total count rate has a large second derivative; presumably this is due to subtracting the 20 s running average.

Simultaneously with the change in modulation frequency at 1544UT, the X-ray spectrum also changes. Figure 1c shows the ratio of the background subtracted count rates between 106 keV and 1.365 MeV to that between 20 and 106 keV (the total event has about equal number of counts above and below 106 keV). Peak 1 corresponds to a relatively hard spectrum, while the following minimum, ~1535 UT, has the softest spectrum in the event. For the peaks 2, 3, and 4 the spectrum becomes progressively harder but the intervening minima are harder than the maxima. At ~1544 UT, the X-ray spectrum abruptly hardens and then stays essentially constant through both maxima and minima for the peaks 5, 6, 7.

The background count spectrum (Figure 2 bottom) before the burst (1430-1530 UT) shows lines at ~75 keV and ~85 keV from K_α and K_β emissions of the lead collimator, at 198 keV from neutron inelastic scattering off ^{71}Ge inside the detector, and at 511 keV from e^+-e^- annihilation of positrons produced by cosmic rays and their secondaries interacting with the atmosphere and instrument. Figure 2 (middle) shows background subtracted count spectra for the burst, before (crosses) and after 1544 UT (diamonds). The ^{71}Ge and e^+-e^- lines are eliminated by the background subtraction, but the lead lines are still present since the enhanced >~100 keV X-ray flux in the burst produces K shell excitation. The spectra before and after 1544 UT differ significantly only above ~160 keV, and both spectra show a significant number of counts up to the instrumental limit of ~1.4 MeV.

The count rate falls off below ~60 keV due to attenuation by the overlying atmosphere. To obtain the photon spectrum at the top of the atmosphere, the absorption and scattering in the instrument and atmosphere is modeled using Monte Carlo simulations (see *Smith et al., 1995*). The atmosphere is modeled as 10 different concentric shells of varying thickness and density. Photons emitted isotropically above the atmosphere are propagated down to the balloon where their angles and energies are recorded. The response of the GeD system, modeled as 20 different regions of material, is then simulated. The result is a set of matrices which yield the GeD response for an arbitrary X-ray energy spectrum at the top of the atmosphere and elevation angle of the source.

Preliminary analysis of the XRI observations *(Lorentzen et al., 1997)* indicate that the source was approximately uniform over XRI's 45° half angle conical aperture, with no significant spatial variability through the burst. The observed count spectrum for the entire event was therefore multiplied by the inverse of the response matrices for a uniform photon distribution over the aperture, to obtain the bremsstrahlung source spectrum (top of Figure 2) at the top of the atmosphere. This

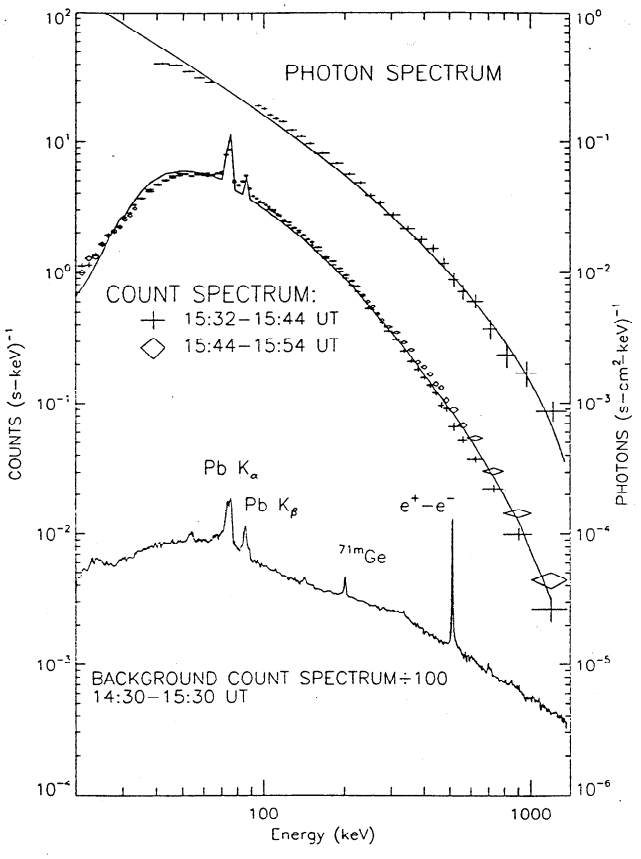

Figure 2. The bottom trace is a background count spectrum (divided by 100) before the event (14:30-15:30 UT). In the middle are event count spectra (background subtracted) for 15:32-15:44 UT (crosses) and 15:44-15:54 UT (crosses with dots). At the top is the source photon spectrum (averaged over the entire event) obtained by removing atmospheric absorption and detector response effects from the measured count spectrum. The curves through the photon spectrum and count spectra are model fits calculated assuming a precipitating electron population that is monoenergetic at 1.7 MeV.

fits a power law spectrum $dJ/dE \propto E^{-\delta}$ with δ=1.6 from $\lesssim$ 100 to 250 keV, steepening to δ = 2.8 above ~ 400 keV. A single exponential [$dJ/dE \propto \exp(-E/E_0)$] does not fit; the e-folding energy E_0 varies from ~ 75 keV at low energies to ~ 400 keV at high energies.

With high resolution measurements of the photon spectrum, the corresponding X-ray producing electron spectrum can be derived by the method of *Johns and Lin [1992]*, in which a response matrix is calculated for the bremsstrahlung emission process and inverted directly. Then, a continuity equation for the electrons can be solved to obtain the precipitating electron population, if the electron loss mechanism (presumably, Coulomb collisions in the atmosphere) is known *[Lin and Johns, 1994]*. When the detailed spatial distribution of the precipitation source becomes available from the XRI, this procedure will be carried out, but in the meantime the observations can be compared to model calculations.

The solid curves through the points in Figure 2 (upper and middle) are the photon and count spectra computed for monoenergetic 1.7 MeV electrons precipitating uniformly over that part of the sky viewed by the GeD. The calculation takes into account electron slowing by collisions, bremsstrahlung production, and atmospheric and instrumental scattering/absorption of the photons. The fit is good except at energies below ~ 100 keV, where the corrections for atmosphere and GeD window absorption are poor, and the neglect of screening effects in the brehmsstrahlung cross section may no longer be valid *(Koch and Motz, 1959)*. Other model precipitating electron spectra were tried, but the spectrum is so hard that the bulk of the precipitating electrons must be at high energies, above ~1-2 MeV. The observed hardening of the spectrum at 1544 UT is consistent with an increase in the peak energy of the precipitating electrons.

During this event, no spacecraft were on the same field line as the balloon, but the trapped electron spectrum between 0.6 and 4 MeV measured by the geosynchronous GOES-9 satellite (L=6.6, 225° East longitude) is steeply falling, with $dJ/dE \propto E^{-5}$. Thus, if the source is the trapped electron population, only the highest energy, > 1-2 MeV electrons, are precipitated. Since precipitating ~1-2 MeV electron can penetrate down to <~55 km altitude *(Berger and Seltzer, 1972)*, only ~20 km above the balloon, the source could be as small as ~40 km diameter and still fill the GeD and XRI apertures.

Using the average precipitating electron flux of J_p~300 $(cm^2\text{-}s)^{-1}$ and the ~2 MeV electron flux of $J_t \sim 4\times10^3$ $(cm^2\text{-}s)^{-1}$ measured at GOES-9, we estimate the mean electron lifetime to be about 10^2 s (see O'Brien 1962). In this time the local flux tube would be replenished several times over by electrons drifting in longitude.

Discussion

Spacecraft observations show that MeV electron precipitation events occur predominantly around local midnight, ~2000 - 0400 MLT. The precipitating electron spectrum is often peaked at MeV energies, possibly due to the magnetic field lines connecting into the magnetotail where their radius of curvature may be small enough to scatter and isotropize the highest energy electrons *(Imhof et al., 1997; Sergeev and Malkov, 1988)*. Afternoon relativistic electron precipitation (REP) events are rare - only six out of 313 REP events observed by the S3-3 satellite *(Thorne and Andreoli, 1980)* - and afternoon field lines are unlikely to extend into the magnetotail.

The observed 10-20s period modulation of the X-rays in this burst suggests the possibility that the relativistic electrons may have been scattered into the loss cone by gyro-resonance with Doppler shifted electromagnetic ion-cyclotron (EMIC) waves *(Thorne and Andreoli, 1980)*. From the dispersion relation and the relativistic resonance condition, the dependence of the resonant electron energy E_r on wave frequency ω is

$$\frac{E_r}{m_e c^2} = \left[1 + \frac{2E_m}{m_e c^2}\left(\frac{m_i}{m_e}\right)\left(\frac{\Omega_i}{\omega}\right)^2\left(1 - \frac{\omega}{\Omega_i}\right)\right]^{1/2} - 1$$

where $E_m = B^2/8\pi n$ is the magnetic energy per particle, n is the ambient plasma density, and Ω_i is the ion cyclotron frequency (here, taken at the equator). For the observed modulations T = $2\pi/\omega$ ~ 20s and 10s, E_r ~2 MeV, and W_i ~ 18 rad/s for protons at L=5.7, we obtain densities n ~ 5.2 x 10^4 and 1.2 x 10^4 cm^{-3}, respectively, a factor of ~10^2 higher than typical for the plasmasphere. For 0^+, Ω_i ~ 1.1 rad/s, and the corresponding densities would be n ~ 150 and 28 cm^{-3}, respectively. In this picture the decrease in T and increase in E_r at 1544 UT could be due to a sudden decrease in plasma density. However, for this magnetically quiet time such high proton densities or substantial 0^+

densities are unlikely. On the other hand, no significant modulation was detected in the burst at the EMIC resonant frequencies (~1 Hz) for normal plasmaspheric densities. The X-ray burst reported by *Parks et al.* (1979) was also detected at L~4.5-5 in the mid-afternoon (~1400 MLT). It also consisted of a series of ~100 sec FWHM peaks separated by ~100-200 sec. Although the highest energy threshold was only ~120 keV, the spectrum was comparably hard below 120 keV, strongly suggesting it was the same type of event as reported here. Whistler perturbations were observed (West and Parks, 1984) which may explain the diffusion of MeV electrons and their subsequent precipitation in both events.

The 2-12 keV channel of the PIXIE X-ray imager (Chenette, private communication) and the UVI imager on the Polar spacecraft detected emissions at 1515 UT (possibly a small substorm intensification) near midnight but not near Kiruna. By 1545 UT, neither instrument detected any precipitation. However, imaging riometer data from Kilpisjärvi in Northern Finland (IRIS) show a clear absorption feature ~100 km(N-S) by ~200 km (E-W) size (at 90 km altitude) over the balloon. The absorption increased at 1535 UT reaching a maximum between 1536-1537 UT and then decreased. It then increases again at about 1544 UT, the same time that the hardening of the X-ray spectrum and change in modulation frequency were observed.

A ULF field line resonance (FLR) was identified from analysis of data from the International Monitor for Auroral Geomagnetic Effects (IMAGE) magnetometer network (Viljanen and Häkkinen, 1997), which includes Kiruna and from the Iceland East coherent scatter HF radar of the Super Dual Auroral Radar Network (SuperDARN) (*Greenwald et al., 1995*). From 1400 to 1700 UT, the power spectra of the IMAGE data showed peaks at a number of discrete frequencies, i.e. 1.3 mHz, 1.8 mHz, 3.8 mHz, and 4.9 mHz, extending over many stations, and SuperDARN identified a 1.6-1.8 mHz FLR from 1545 to 1645 UT. The 4.9 mHz FLR, whose period is comparable to the peak spacing of the X-ray burst, was observed at all stations from 57° to 75° magnetic latitude with peak power at 65.9°. We speculate that a disturbance related to the FLR may have triggered motion of the plasmasphere boundary and/or detachment of plasma. How this led to resonant scattering of MeV electrons into the loss cone is presently unknown.

Acknowledgments. The research at University of California, Berkeley, and University of Washington was supported by NSF grant ATM 9221612 in 1996-7. In 1998, UCB was supported by NASA grant NAG5-6870 and UW by NSF grant ATM 9223612. Greg Zimmer at UCB and John Chin at UW provided electronics support. The research at CESR/CNRS and Université Paul Sabatier was supported by CNES grant 96CNES208 and the balloon campaign was managed by CNES who provided balloons and careful lauchings from Esrange, Sweden. The SuperDARN observations were provided by SuperDARN team and the IMAGE magnetometer data used in this paper were collected as a German-Finnish-Norwegian-Polish project conducted by the Finnish Meteorogical Institute. The riometer data originated from the Imaging Riometer for Ionospheric Studies (IRIS), operated by the Communications Research Centre at Lancaster University (UK), funded by the Particle Physics and Astronomy Research Council (PPARC) in collaboration with the Sodankylä Geophysical Observatory.

References

Anderson, K. A., Balloon measurements of X-rays in the auroral zone, in *Auroral Phenomena*, edited by M. Walt, p. 46, Stanford Univ. Press, Stanford Calif, 1965.

Anderson, K. A. and D. E. Enemark, Balloon observations of X-rays in the auroral zone, II, *J. Geophys. Res.*, **65**, 3521, 1960.

Baker, D. N., J. B. Blake, D. J. Gorney, P. R. Higbie, R. W. Klebesadel, and J. H. King, *Geophys. Res. Lett.*, **14**, 1027, 1987.

Berger, M.J., and S.M. Seltzer, Bremsstrahlung in the atmosphere, *J. Atmos. and Terrestrial Phys.* **34**, 85, 1972.

Blake, J. B., M. D. Looper, D. N. Baker, R. Nakamura, B. Klecker, and D. Hovestadt, New high temporal and spatial resolution measurements by SAMPEX of the precipitation of relativistic electrons, *Adv. Space Res.*, **18**, 8171, 1996.

Evans, D. S., A pulsating auroral-zone X-ray event in the 100 second period range, *J. Geophys. Res.*, **68**, 395, 1963.

Greenwald, R. A., K. B. Baker, J. R. Dudeny, M. Pinnock, T. B. Jones, E. C. Thomas, J.-P. Villain, J. -C. Cerisier, C. Senior, C. Hanuise, R. D. Hansucker, G. Sofko, J. Koehler, E. Nielson, R. Pellinen, A. D. M. Walker, N. Sato and Y. Yamagishi, DARN/SuperDARN A global view of the dynamics of high-latitude convection, *Space Sci. Rev.*, **71**, 761, 1995.

Imhof, W.L., G.H. Nakano, and J.B. Reagan, Satellite observations of impulsive bremsstrahlung X-ray events associated with substorms, *J. Geophys. Res.*, **83**, 4237, 1978.

Imhof, W. L., H. D. Voss, J. Mobilia, D. W. Datlowe, E. E. Gaines, The precipitation of relativistic electrons near the trapping boundary, *J. Geophys. Res.*, **96**, 5619, 1991.

Imhof, W. L., D.L. Chenette, E.E. Gaines, and J.D. Winningham, Characteristics of electrons at the trapping boundary of the radiation belts, *J. Geophys. Res.*, **102**, 95, 1997.

Johns, C. M. and R. P. Lin, The derivation of parent electron spectra from bremsstrahlung hard X-ray spectra, *Solar Phys.*, **137**, 121, 1992. (*Erratum, Solar Phys.*, **142**, 219, 1992.)

Koch, H. W., and J. W. Motz, Bremsstrahlung cross-section formulas and related data, *Rev. Mod. Phys.*, **31**, 920, 1959.

Lin, R.P., and C. M. Johns, Two accelerated electron populations in the 1980 June 27 Solar Flare, *Ap. J. Letter*, **417**, L53, 1993.

Lorentzen, K.R., M.P. McCarthy, G.K. Parks, R.P. Lin, J.E. Foat, D. Smith, J.P. Treilhou, Balloon-born X-ray imager observations of dayside relativistic electron precipitation, EOS, *Transactions American Geophysical Union*, **78**, 595, 1997.

O'Brien, B.J., Lifetimes of outer zone electrons and their precipitation into the atmosphere, *J. Geophys. Res.* **67**, 3687, 1962.

Parks, G. K., C. Gurgiolo, and R. West, Relativistic electron precipitation, *Geophys. Res. Lett.*, **6**, 393, 1979.

Parks, G. K., D. W. Milton, and K. A. Anderson, Auroral zone X-ray bursts of 5 to 25 millisecond duration, *J. Geophys. Res.*, **72**, 4587, 1967.

Parks, G. K., T. J. Freeman, M. P. McCarthy, and S. H. Werden, The discovery of auroral X-rays by balloon-borne detectors and their contributions to magentospheric research, Auroral Plasma Dynamics, *Geophysical Monographs*, **80**, 17, 1993.

Sergeev, V.A., and M.V. Malkov, Diagnostics of plasma sheet magnetic configuration based on energetic electron measurements above the ionosphere, *Geomag. Aeron.*, Engl. Trans., **28**, 649, 1998.

Smith, D. M., R. P. Lin, K. A. Anderson, K. Hurley, and C. M. Johns, High-resolution spectra of 20-300 keV hard X-rays from electron precipitation over Antarctica, *J. Geophys. Res.*, **100**, 19,675, 1995.

Thorne, R. M., and L. J. Andreoli, Mechanisms for intense relativistic electron precipitation, in *Exploration of the Polar Upper Atmosphere*, ed. C.S. Deehr and J.A. Holtet, pub. D. Reidel, p.381, 1980.

Viljanen, A. and L. Hakkinen, 1997: IMAGE magnetometer network. In: Satellite-Ground Based Coordination Sourcebook (eds. M Lockwood, M.N. Wild and H.J. Opgenoorth). ESA publications SP-1198, p. 111-117.

West and Parks, ELF Emissions and Relativistic Electron Precipitation, *J. Geophys. Res.*, **89**, 159-167, 1984.

Winckler, J. R., L. Peterson, R. Arnoldy, and R. Hoffman, X-rays from visible aurorae at Minneapolis, *Phys. Rev.*, **110**, 1221, 1958.

(Received August 20, 1998; accepted September 28, 1998.)